Ising-Type Magnetic Anisotropy in a Cobalt(II) Nitronyl Nitroxide Compound: A Key to Understanding the Formation of Molecular Magnetic Nanowires

A. Caneschi,[a] Dante Gatteschi,*[a] N. Lalioti,[a] R. Sessoli,[a] L. Sorace,[a] V. Tangoulis,[a] and A. Vindigni[b]

Abstract: The compound [Co(hfac)$_2$(NITPhOMe)$_2$] (**2**) (hfac = hexafluoroacetylacetonate, NITPhOMe = 4′-methoxyphenyl-4,4,5,5-tetramethylimidazoline-1-oxyl-3-oxide) crystallizes in the triclinic $P\bar{1}$ space group, $a = 10.870(5)$, $b = 11.520(5)$, $c = 19.749(5)$ Å, $\alpha = 78.05(5)$, $\beta = 84.20(5)$, $\gamma = 64.51(5)^\circ$, $Z = 2$. It can be considered a model system for studying the nature of the magnetic anisotropy of [Co(hfac)$_2$(NITPhOMe)] (**1**), which was recently reported to behave as a molecular magnetic wire. The magnetic anisotropy of **2** was investigated by EPR spectroscopy and SQUID magnetometry both in the polycrystalline powder and in a single crystal. The experimental magnetic anisotropy was related to the anisotropy of the central ion and to the exchange interaction between the cobalt(II) ion and the radicals.

Keywords: angular overlap model · cobalt · magnetic properties · radicals

Introduction

Molecular magnetism provides a range of exciting new types of magnets[1] that are attracting increasing interest, both for fundamental science and for the development of new unconventional applications. A particularly novel field is provided by molecular clusters that show slow relaxation of the magnetization at low temperatures, and which give rise to magnetic hysteresis of molecular origin.[2] These materials can be considered to be magnetic analogues of quantum dots in conductors, in the sense that they are zero-dimensional in nature and show properties similar to those of bulk magnets (slow relaxation of the magnetization) accompanied by important quantum effects.[3–5] To design and synthesize new materials with implemented properties to store information on the nanometer scale, it is necessary to have clear indications for the requirements needed to observe slow relaxation of the magnetization at low temperatures. It is now well-known that the principal requisite corresponds to a negative zero-field splitting parameter D in the ground S state, which must be as large as possible. This corresponds to an easy axis (Ising)-type anisotropy.

A possible approach to obtain slowly relaxing magnetic clusters is the use of individual building blocks that have large zero-field splittings and z axes that are mutually parallel. The importance of this last requirement has been clearly shown in the case of the isomeric forms of well-known Mn$_{12}$ clusters. In fact, these clusters contain eight manganese(III) and four manganese(IV) ions. The former have Jahn–Teller distortions that provide an Ising-type magnetic anisotropy. In the archetypal [$Mn_{12}O_{12}(CH_3COO)_{16}(H_2O)_4$], the unique manganese(III) axes are essentially parallel to each other,[6] giving rise to a zero-field splitting $D/k = -0.70$ K. Two isomeric forms of [$Mn_{12}O_{12}(p\text{-MeBz})_{16}(H_2O)_4$] show a different orientation of the elongation axes of manganese(III) and quite distinct relaxation rates.[7, 8] In principle, Ising-type magnetic anisotropy also influences the relaxation of one-dimensional magnets, as suggested by Glauber in the 1960s.[9] According to Glauber's theory, an Ising chain should show exponential divergence of the relaxation time of the magnetization as the temperature decreases. The temperature-dependence of the relaxation time should depend on a barrier proportional to the exchange coupling constant. Although this theory has been known for more than forty years it had never been tested because very strong intrachain and very weak interchain interactions are required in addition to the Ising anisotropy.

We recently reported that the chain compound [Co(hfac)$_2$(NITPhOMe)] (**1**) (where hfac = hexafluoroacetylacetonate and NITPhOMe = 4′-methoxyphenyl-4,4,5,5-tetramethylimidazoline-1-oxyl-3-oxide, is composed of cobalt(II) ions and nitronyl nitroxide radicals alternately arranged in a trigonal helix.[10] The spin of the metal ion and that of the radical are strongly interacting and below 20 K the a.c. susceptibility

---

[a] Prof. D. Gatteschi, Dr. A. Caneschi, Dr. N. Lalioti, Prof. R. Sessoli, Dr. L. Sorace, Dr. V. Tangoulis
Dipartimento di Chimica
Università degli Studi di Firenze and INSTM, U.d.R. Firenze
50144 Firenze (Italy)

[b] Dr. A. Vindigni
Istituto Nazionale per la Fisica della Materia, Unità di Firenze
50125, Firenze (Italy)

shows the appearance of an out-of-phase signal that is strongly dependent on the frequency, as observed in molecular clusters.[11] The relaxation time follows the Arrhenius law in a wide range that covers almost ten orders of magnitude, providing a spectacular example of Glauber dynamics.[12] Furthermore, the compound exhibits magnetic hysteresis in the absence of three-dimensional magnetic order. The chains behave as magnetic wires, and, in principle, it may become possible to store information on a single polymeric chain. The Ising nature of the chain has been attributed to the presence of cobalt(II) as this ion is known to yield large anisotropy effects when it is hexacoordinated.[13] Tetragonal elongation and trigonal compression provide Ising-type anisotropy; however, in lower symmetry the anisotropy is hardly predictable. Within the chain, the local anisotropy of the cobalt ions is mediated by the helical structure so that unambiguous estimation of the anisotropy of cobalt has not been possible.

We have now synthesized the mononuclear cobalt(II) bis-nitronyl-nitroxide derivative $[Co(hfac)_2(NITPhOMe)_2]$ (**2**) in which the metal ion has essentially the same coordination geometry as observed in the chain. The quantitative analysis of the magnetic properties of cobalt(II) exchange-coupled systems is not trivial and sophisticated techniques, such as inelastic neutron scattering, have recently been used to quantify the magnetic interactions within a pentameric cobalt(II) cluster.[14] Herein we have investigated **2** in detail by single-crystal EPR spectroscopy and single-crystal magnetization measurements. The anisotropy parameters have been accurately determined so that light can be shed on the nature of the exchange interaction and of the anisotropy in the one-dimensional compound **1** and it also provides useful hints for designing new molecular magnetic materials with higher blocking temperatures.

Results

Synthesis and molecular structure: The system $[Co(hfac)_2]$/NITPhOMe results in two different well-characterized crystalline derivatives according to the experimental conditions. If the ratio of $[Co(hfac)_2]$/NITPhOMe is 1:1 and the solution in *n*-heptane is warmed to 80 °C or higher, the product that quickly precipitates is the helical polymer $[Co(hfac)_2(NITPhOMe)]$ (**1**). With the same stoichiometric ratio but with a lower reaction temperature, ≈60 °C, the mononuclear compound $[Co(hfac)_2(NITPhOMe)_2]$ (**2**) is formed in a mixture with the excess of the cobalt starting material. When **1** was recrystallized in all the solvents investigated, the mononuclear complex **2** was always formed. This suggests that **2** is thermodynamically favored over to the chain compound **1**. Complex **2** crystallizes in the triclinic space group $P\bar{1}$. The structure contains octahedrally coordinated cobalt(II) ions with four oxygen atoms from two hfac molecules and two oxygen atoms from two *cis*-coordinated NITPhOMe radicals (Figure 1). The coordination polyhedron of each Co(II) ion is rather distorted with Co–O bond lengths ranging from 2.030(3) to 2.109(3) Å ($Co{-}O_{rad} = 2.057(3)$ and 2.109(3) Å, respectively). The maximum distortion from octahedral symmetry is observed in the O2-Co-O3 angle, which is 163.60(12)°, while the angle between the two coordinated O atoms of the radicals O5-Co-O6 is 84.02(11)°. This distortion can be explained by the *cis* coordination and by the π-stacking interactions between the phenyl ring of the NITPhOMe radical and the unsaturated part of one of the hfac molecules, as previously observed in other $[M(hfac)_2NITR]$ compounds.[10]

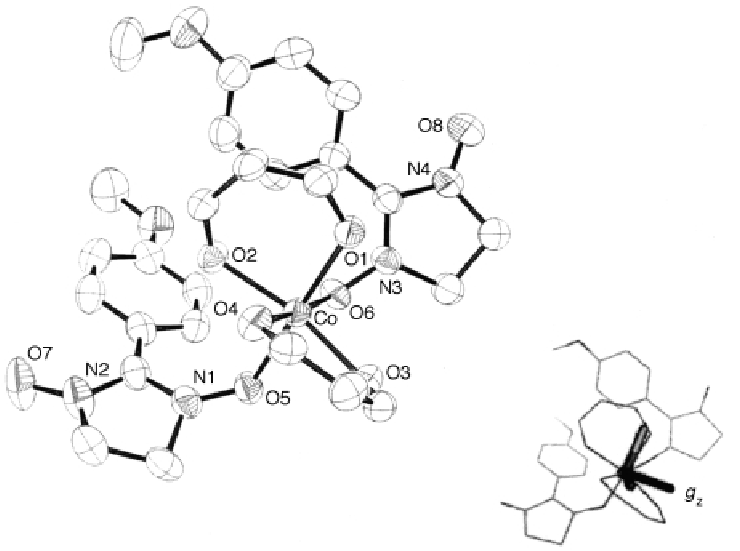

Figure 1. Structure of **2** (ORTEP view). For the sake of clarity, the hydrogen atoms, as well as the methyl and the CF_3 groups have been omitted. The principal directions of the ***g*** tensor of the trimer are shown with respect to the molecular structure. The direction of g_y and g_x are represented in gray with decreasing darkness, while the g_z direction has been labeled.

The basic architecture of **2** compares well with that found in **1**: the radicals bridge two different metal ions to form a trigonal helix. The two coordination polyhedra are compared in Figure 2, which is important with respect to the discussion of the magnetic properties.

In the case of the monomer, π stacking occurs between the phenyl ring (C24–C29) and one hfac ligand (O1–O3) without formation of the "sandwich" structure observed in **1** (Figure 2). The stacking interactions between the corresponding planes are characterized by the angle $\beta = 12.6°$ and the distance $d = 3.5$ Å.[15] Selected bond lengths and angles are given in Table 1. No significant intermolecular contacts are observed. The shortest distance between noncoordinated NO groups is 6.58 Å.

EPR spectra: Polycrystalline powder EPR spectra of **2** at X-band frequency were observed at temperatures below 40 K.

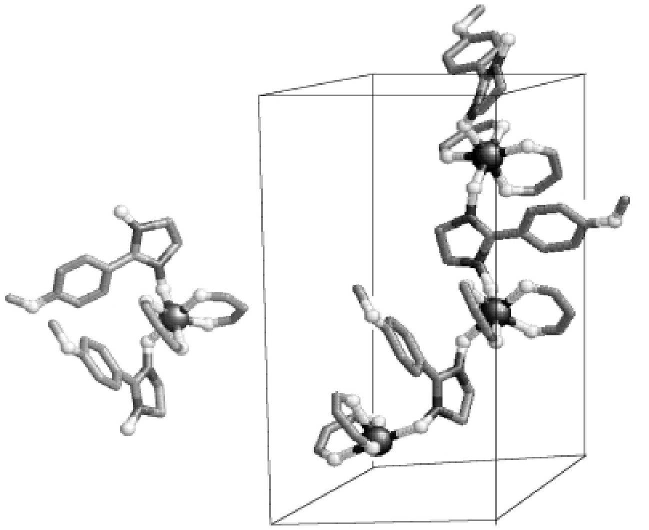

Figure 2. Comparison of the molecular structure and coordination environment of the cobalt ion in the monomeric **2** (left) and chain compound **1** (right).

Table 1. Selected bonds lengths [Å] and angles [°] for **2** compared to those found in **1**.[a]

2		**1**	
Co1 – O3 2.030(3)	N1 – C13 1.357(5)	Co1 – O6 2.028(4)	N9 – C17 1.337(8)
Co1 – O2 2.038(3)	N2 – O7 1.278(5)	Co1 – O5 2.040(4)	N8–O3 1.300(6)
Co1–O6 2.057(3)	N2–C13 1.353(5)	Co1–O4 2.057(5)	N8–C17 1.366(7)
Co1–O1 2.064(3)	N3–O6 1.310(4)	Co1–O7 2.086(5)	
Co1–O4 2.108(3)	N3–C23 1.333(5)	Co1–O3 2.097(4)	
Co1–O5 2.109(3)	N4–O8 1.269(4)	Co1–O2* 2.108(4)	
N1–O5 1.295(4)	N4–C23 1.358(5)	N9–O2 1.287(6)	
O3-Co1-O2 163.60(12)	O2-Co1-O5 89.93(11)	O6-Co1-O5 166.60(2)	O7-Co1-O3 99.13(2)
O3-Co1-O6 97.57(12)	O6-Co1-O1 89.73(11)	O6-Co1-O4 94.95(2)	O2*-Co1-O6 95.46(2)
O3-Co1-O1 95.52(11)	O6-Co1-O4 174.18(10)	O6-Co1-O7 85.82(2)	O2*-Co1-O4 87.59(2)
O3-Co1-O4 85.19(11)	O6-Co1-O5 84.02(11)	O6-Co1-O3 84.29(2)	O2*-Co1-O7 175.57(2)
O3-Co1-O5 86.19(11)	O1-Co1-O4 84.89(11)	O5-Co1-O4 89.99(2)	O2*-Co1-O3 85.28(2)
O2-Co1-O6 97.86(11)	O1-Co1-O5 173.69(11)	O5-Co1-O7 81.90(2)	O2*-Co1-O5 97.16(2)
O2-Co1-O1 90.06(11)	N1-O5-Co1 122.33(2)	O5-Co1-O3 92.35(2)	N8-O3-Co1 127.34(4)
O2-Co1-O4 79.95((11)	N3-O6-Co1 123.70(2)	O4-Co1-O7 88.05(2)	N9*-O2*-Co1 129.73(4)
O4-Co1-O1 101.32(11)		O4-Co1-O3 172.70(2)	

[a] The correspondence in the labeling of atoms between the monomer **2** and the chain **1** derivatives is the following: O1(**2**) → O4(**1**), O2 → O5, O3 → O6, O4 → O7, O5 → O3, O6 → O2. * denotes the atoms in the helix generated by the threefold screw axis.

They correspond to an $S = 1/2$ spin in a rhombic environment (Figure 3). A simple inspection of the spectra suggests the following g values: $g_1 = 3.0$, $g_2 = 2.3$, $g_3 = 1.8$. The three features are characterized by remarkably different linewidths. In particular, the high-field feature has a very broad shape, suggesting that unresolved hyperfine interactions may be present.

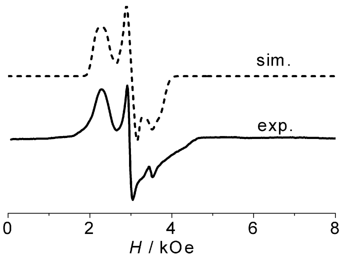

Figure 3. Observed (bottom) and computer-simulated (top) EPR spectrum of polycrystalline powder of **2** at 7 K and at X-band frequency. For the simulation we used: $g_x = 1.85$, $g_y = 2.2$, $g_z = 2.9$, $A_x = 50$ G, $A_y = 30$ G, and $A_z = 70$ G.

Assuming that unresolved hyperfine interactions may be operative, the spectra were simulated with the spin Hamiltonian given in Equation (1), where $I = 7/2$ is the nuclear spin of ^{59}Co.

$$H = \sum_{i=x,y,z} \mu_B H g_i S_i + \sum_{i=x,y,z} A_i S_i I_i \qquad (1)$$

The simulated spectrum shown in Figure 3 was obtained with the following parameters: $g_1 = 2.9$, $g_2 = 2.2$, $g_3 = 1.85$, and $A_1 = 70$ G, $A_2 = 30$ G, $A_3 = 50$ G, with anisotropic linewidths ($W_1 = 160$ G, $W_2 = 100$ G, $W_3 = 210$ G). The hyperfine contribution of the nitrogen atoms of the radicals have not been taken into account. The quality of the fit is moderately satisfactory, but the main features are reproduced.

Single-crystal EPR measurements were performed on **2**. A single crystal was oriented with the same diffractometer used for the structure determination. This crystal had the shape of a platelet with the faces (0,0, ± 1) largely developed and bounded by the (0, ± 1, ± 1) and (± 1, ± 1,0) faces. Single-crystal EPR spectra were recorded during rotation of the crystal around the three orthogonal axes a, b', and c^* (where a is the crystallographic axis, c^* is the normal to the (0,0,1) face, and b' is orthogonal to the first two axes). The spectra in most orientations show one signal whose resonance field and linewidth have strong angular dependence (Figure 4). In some orientations, the signal shows some evidence of splitting, with the appearance of a shoulder at the resonance field, as often observed when unresolved hyperfine interactions are present. In some orientations, weak satellites are also observed. By increasing the temperature,

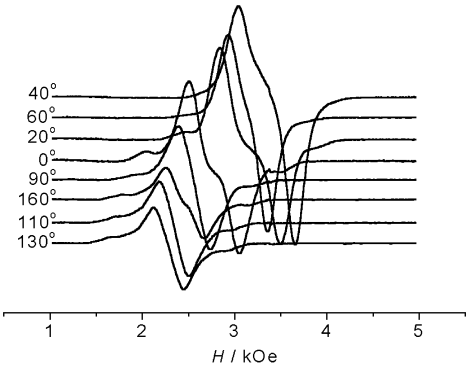

Figure 4. Angular dependence of the single-crystal EPR signal of **2** observed by rotating about the c^* crystallographic axis at 4.2 K. At $\theta = 0°$, the field is along the crystallographic a axis.

0947-6539/02/0801-0288 $ 17.50+.50/0

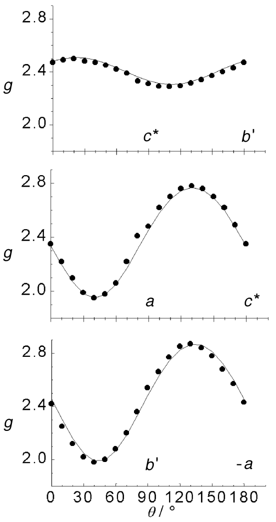

Figure 5. Angular dependence of the g values of **2** extracted from the position of the main line in the single-crystal EPR spectra recorded by rotating about the a (top), b' (middle), and c^* (bottom) crystallographic axes. The lines correspond to the values calculated with the diagonalization procedure (see text) which gives the results reported in Table 2.

the signals dramatically broaden and the compound is EPR silent above 40 K. This is in agreement with the presence of cobalt(II) ions which are known to relax rapidly at high temperatures.[16]

The angular dependence of the g value of the main line is shown in Figure 5. The minimum g was observed in the rotation b' at ≈40° from c^*, while the maximum g was observed in the rotation around c^* at ≈130° from a. The principal values and directions of the $\boldsymbol{g}$ tensor were determined by standard least-squares analysis[17] and are given in Table 2 (the uncertainty in the angles is ±5°). The principal direction associated with the minimum g value lies 17.8° from the Co–O1 bond and 12.7° from the normal to the O3-C6-C7-C8-O4 hfac plane, while the direction associated with the maximum g is approximately between the Co–O1 and Co–O6 bonds, as shown in Figure 1. The principal values of the $\boldsymbol{g}$ tensor estimated from the single-crystal spectra are in reasonable agreement with those evaluated from the powder spectrum.

A more detailed analysis of the single-crystal spectra would require the inclusion of hyperfine interactions and of the interactions responsible for the observed splitting of the lines. The latter are presumably caused by dipolar interactions between neighboring molecules, which are of the same order of magnitude as the hyperfine splitting. Similar effects were previously observed in magnetically undiluted copper(II) compounds.[18] In the present case, the detailed analysis is complicated by the large number of lines present (8 hyperfine lines, each split into a number of fine structure lines, which depend on the number of neighbors). Furthermore, no really well-resolved spectra were observed. Therefore, we limited our investigation to obtain reliable values of g and as well as its principal directions. The simulation of the single spectra starting from the values reported in Table 2 and taking into account the hyperfine structure is satisfactory, except for those orientations where the satellites are more intense.

Table 2. Principal values and cosine directors in the $ab'c^*$ reference frame of the $\boldsymbol{g}$ tensor of **2** at 4.2 K.

$g_z = 2.998$	−0.694
	0.577
	−0.429
$g_y = 2.332$	−0.116
	−0.678
	−0.725
$g_x = 1.790$	0.710
	0.454
	−0.538

Magnetic measurements: The χT value for polycrystalline powders of **2**, pressed in a pellet to avoid orientation in the external field, is 1.25 emu K mol^{-1} at room temperature. This is well below the value expected for uncorrelated spins (2.625 emu K mol^{-1} if all the g values were equal to 2). Since high-spin cobalt(II) has a positive orbital contribution to g, it is apparent that the low value of χT can only be justified by strong antiferromagnetic interactions between cobalt(II) and the radicals. χT decreases on lowering the temperature and levels out at ≈0.7 emu K mol^{-1} at low temperatures.

Single-crystal magnetic measurements were performed at 2–40 K by orienting the crystal with its principal directions x, y, and z of the $\boldsymbol{g}$ tensor, as determined from the EPR spectra, parallel to the magnetic field of the SQUID magnetometer (the largest error in the orientation was estimated to be ±10°). As expected, the magnetization is highly anisotropic (Figures 6 and 7). The χT values reported in Figure 6 are practically independent of temperature in all three directions, with a small decrease at the lowest temperature. The observed values (0.82 emu mol^{-1} K for z, 0.56 emu mol^{-1} K for y, and 0.34 emu mol^{-1} K for x) are in reasonable agreement with what would be expected for a system of noninteracting $S = 1/2$ spins, with the g values observed in the EPR spectra (0.84, 0.52, and 0.30 emu mol^{-1} K, respectively). The fact that the χT

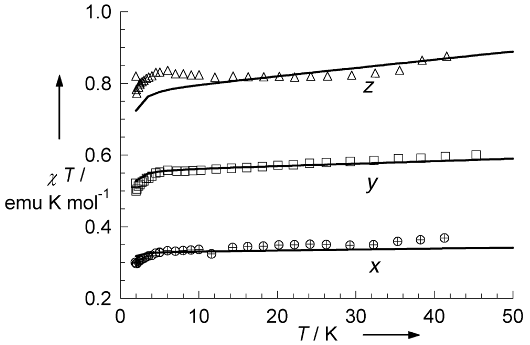

Figure 6. Temperature dependence of the magnetic susceptibility multiplied by the temperature measured on a single crystal of **2** with the magnetic field oriented along the direction of largest (z), intermediate (y), and smaller (x) component of the $\boldsymbol{g}$ tensor, as determined from the EPR spectra. The lines correspond to the calculated values (see text).

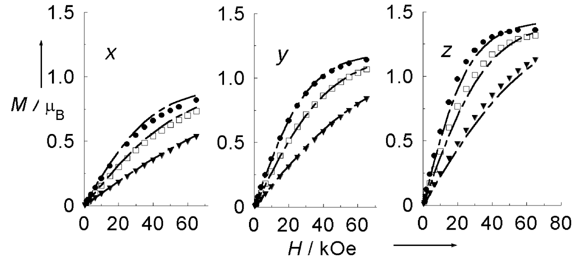

Figure 7. Field dependence of the molar magnetization of a single crystal of **2** with the magnetic field oriented along the direction of largest (z), intermediate (y), and smaller (x) component of the $\boldsymbol{g}$ tensor, measured at 2 K (●), 3.5 K (□), and 6 K (▽). The lines correspond to the calculated values (see text).

values are essentially independent of temperature suggests that the $S = 1/2$ ground state is the only one which is thermally populated up to 40 K.

The magnetization versus applied field spectrum, with the field oriented along the three principal axes, has been measured at 2.5, 3.5, and 6 K; the results are shown in Figure 7. The curves display an approach to saturation with values in reasonable agreement with those expected for $S = 1/2$ with the same g values as extracted from EPR spectroscopic measurements.

Discussion

The analysis of the magnetic properties of compounds that contain octahedral cobalt(II) is hampered by the presence of largely unquenched orbital contributions associated with the ground $^4T_{1g}$ state. Low-symmetry components and spin-orbit coupling effects remove the degeneracy leaving one Kramers doublet lying at the lowest level, separated from the excited states by more than 100 cm^{-1}. Therefore, it is a reasonable approximation to treat the cobalt(II) ion at low temperatures as an effective $S = 1/2$, corresponding to the Kramers doublet, with high anisotropy. The magnetic coupling can therefore be expressed by the Hamiltonian given in Equation (2).

$$H = J_z S_{1z} S_{2z} + J_x S_{1x} S_{2x} + J_y S_{1y} S_{2y} \tag{2}$$

When $J_z \mp 0, J_x = J_y = 0$, the system is at the Ising limit, when $J_z = 0$, $J_x = J_y \mp 0$ the system is at the XY limit. Important information on the nature of the exchange interaction is obtained from the g values of the cobalt(II) ions: for $g_z > g_x, g_y$ the system is closer to the Ising limit, for $g_x, g_y > g_z$ the system is closer to the XY limit.

The conditions for observing $g_z > g_x, g_y$ were given at an early stage by Abragam and Bleaney[13] by means of a crystal-field approach. This was later generalized by the Florence group who used the ligand-field model.[19, 20] At the Ising limit, $g_z = 8-9$, $g_x = g_y = 0$.

The g values observed in **2** clearly depend on the g values of the cobalt(II) and radical centers, and on the nature of the exchange interaction. Simple formulae are available that relate the individual $\boldsymbol{g}$ tensors to those of the coupled triad at the limit of strong isotropic exchange; however, it is doubtful that such an approximation is valid in this case.

The principal directions of the $\boldsymbol{g}$ tensor are determined by those of g_{Co} because the radicals can reasonably be assumed to have isotropic $\boldsymbol{g}$ tensors. It was previously observed that the $\boldsymbol{g}_{Co}$ tensors are extremely sensitive to low-symmetry components of the ligand field, and that even small deviations from rigorous symmetry determine dramatic deviations of the principal axes from the bond directions, or from their bisectors. Large deviations from idealized symmetries were previously observed in *trans*-[Co(hfac)$_2$X$_2$] derivatives,[21] in which the z axis deviates from the perpendicular of the [Co(hfac)$_2$] plane by as much as 19°, depending on the nature of the axial ligand. Similar large deviations have been observed for the in-plane axes.

Attempts were made to reproduce the field dependence of the anisotropic magnetization and the low-temperature ($T <$ 40 K) dependence of the anisotropic χT value by exact diagonalization of the Hamiltonian given in Equation (3).

$$\begin{aligned} H = {} & J_z(S_z^{Co} S_z^{R1} + S_z^{Co} S_z^{R2}) + J_y(S_y^{Co} S_y^{R1} + S_y^{Co} S_y^{R2}) \\ & + J_x(S_x^{Co} S_x^{R1} + S_x^{Co} S_x^{R2}) + \mu_B \bar{S}^{Co} \boldsymbol{g}^{Co} \bar{H} + \mu_B \bar{S}^{R1} \boldsymbol{g}^{R1} \bar{H} + \mu_B \bar{S}^{R2} \boldsymbol{g}^{R2} \bar{H} \end{aligned} \tag{3}$$

Beyond the three J_i values ($i = x, y, z$), it is necessary to assume that the g values of the cobalt(II) are also parameters, which leaves the $\boldsymbol{g}$ tensors of the radicals as isotropic with $g = 2.00$. The interaction of the cobalt(II) ions with the two radicals was assumed to be identical to avoid over-parameterization. The parameters were allowed to vary in a wide range. Isotropic values of the spin Hamiltonian were unable to reproduce the experimental data, and a large anisotropy was required with a strong antiferromagnetic J_z. The best-fit results are shown as lines in Figures 6 and 7. A very large value, $J_z/k = 3200$ K, was used; however, it must be remarked that the fit can only be performed in the low-temperature range and is therefore essentially insensitive to this value provided that $J_z/k >$ 400 K. The other parameters are: $J_x/J_z = 0(\pm 0.05)$, $J_y/J_z = 0.69(\pm 0.05)$, $g_{zCo} = 9.1(\pm 0.5)$, $g_{yCo} = 0.5$ (± 0.7), and $g_{xCo} = 0$ $(\pm 1.)$. The g values of the cobalt(II) ion evaluated from the fitting are in the high limit of those expected by the Abragam and Bleaney model.[13]

The strong anisotropy of the magnetic interaction suggested by the best-fit parameters implies that the ground-state doublet is not a pure $S = 1/2$ spin state. Nevertheless, the Zeeman splitting, ΔE, of the ground doublet calculated with the above parameters provides the field for which $\Delta E = h\nu$ where ν is the frequency of the EPR experiments. The g values estimated from the calculated resonance field are $g_x = 1.87$, $g_y = 2.43$, and $g_z = 2.87$. They are in reasonable agreement with the result of the single-crystal EPR spectra, displayed in Table 2.

To explain the anisotropic characteristic of the cobalt ion in **2**, as derived from both EPR and magnetic measurements, we employed the angular overlap model. The calculation was performed with a program which has been described elsewhere.[22] Indeed, during past years, the angular overlap approach has been widely used to rationalize the magnetic properties of low-symmetry high-spin cobalt(II) compounds,[20] because low-symmetry effects of the π-interactions can be taken into account in a careful manner. In fact, g anisotropy for distorted octahedral cobalt(II) complexes is mainly dependent on the relative splitting of the t_{2g} orbitals. The π interactions, which can be bonding or antibonding in nature depending on the relative energies of the metal and ligand orbitals, are then crucial in the determination of this splitting. As an example, we may consider a tetragonal coordination environment. In this case, if the splitting of the t_{2g} orbitals results in a ^2E_g ground doublet, then $g_{\parallel} > g_{\perp}$, whereas the reverse applies if the ground doublet is $^2A_{2g}$. In terms of the ligand field approach, the value of the splitting of the t_{2g} orbitals is $\Delta = E(d_{xy}) - E(d_{xz})$, which in the angular overlap formalism may be written as $\Delta = 4e\pi_{\perp eq} - 2e\pi_{\parallel eq} - e\pi_{ax}$.[16] It is then clear that the anisotropy of the π interaction has to be

0947-6539/02/0801-0290 $ 17.50+.50/0

carefully considered in order to understand the magnetic behavior of these systems.

The coordination geometry employed for the calculation was that derived from the solution of the crystal structure, assuming the orthogonalized reference system $ab'c^*$. However, to avoid the use of too many parameters, we did not take into account the variation in bond lengths and thus assumed the same Dq value for the same class of ligand. As initial guesses for the ligand field parameters, we used for the hfac ligand the values which are reported in the literature for acetylacetonate and those of pyridine-*N*-oxide for the nitronyl-nitroxide radicals. The only relevant source for the π anisotropy was readily identified in the radicals, whose interaction could reasonably be assumed to be mainly directed out-of-plane. The anisotropy of this π interaction was then assumed to be quite large ($e_{\pi\parallel}/e_{\pi\perp} = 0.1$). With these starting values, we obtained the following g values for the ground doublet: $g_x = 1.39$, $g_y = 1.97$, and $g_z = 7.21$ which therefore provides evidence for the Ising behavior of the system. We then performed different calculations allowing $e_{\pi\parallel}/e_{\pi\perp}$ for radicals, and e_σ, e_π/e_σ, and e_π for both the two class of ligands to vary by 30% around their starting values. The largest Ising character was obtained on lowering the ratio e_π/e_σ for the radicals down to 0.15. This yielded the following g values: $g_x = 1.43$, $g_y = 1.84$, and $g_z = 7.8$. Finally, as the g values obtained with all the calculations were within the limits $g_x \leq 1.5$, $g_y \leq 1.99$, and $g_z \geq 7.1$, we may conclude that the Ising behavior of cobalt(II) in this system is well accounted for within the framework of the angular overlap model.

Conclusion

The combined use of single-crystal EPR spectroscopy and single-crystal SQUID magnetometry, even in the absence of any symmetry, has allowed an accurate estimation of the magnetic anisotropy of **2**. The cobalt(II) ion coordinated by NITR radicals has Ising-type anisotropy, which gives rise to Ising-type antiferromagnetic exchange interaction between the metal ion and the radicals. This might be a general feature of the cobalt(II)–radical interaction because it seems to be associated with the nature of the π interaction between the metal ion and the radical orbitals.

In molecular magnetism, so far only limited attention has been given to the problem of magnetic anisotropy. However, recent results have shown that the use of highly anisotropic metal ions can introduce new interesting properties in molecular magnets, such as strong coercive fields in bulk magnets,[23] and slow relaxation of the magnetization in zero-dimensional[2] and one-dimensional materials.[11, 12] For the last case in particular, the close resemblance of the cobalt environment in **1** and **2** allows us to confirm that the magnetic anisotropy of the cobalt(II) ions in **1** is of the Ising type as required to observe slow dynamics of the magnetization according to the Glauber model. Moreover, it is possible to overlap the very similar coordination spheres of the cobalt ion in **1** and **2**. Hence the principal directions of the $\boldsymbol{g}$ tensor of **2** suggest that the easy magnetization axis z of each cobalt spin in **1** forms an angle of ≈50° (±10°) with the symmetry axis of the helix. The non-colinearity of the local z axis is an important feature in determining the magnetic properties of **1**.[12] We have shown how the detailed analysis of the anisotropic magnetic properties of simple model systems, such as **2**, may indeed provide some clues for the design of new classes of molecular magnetic materials.

Experimental Section

Synthesis of [Co(hfac)$_2$(NITPhOMe)$_2$]: A solution of NITPhOMe, prepared as previously described,[24](0.13 g, 0.5 mmol) in *n*-heptane (20 mL) was added to a solution of [Co(hfac)$_2$]·2H$_2$O (0.13 g, 0.25 mmol) in CHCl$_3$ (3 mL). Slow evaporation of the final dark blue solution at room temperature gave large (<5 mg), dark blue crystals of **2**, which were suitable for X-ray analysis. Elemental analysis (%) calcd for $C_{38}F_{12}CoH_{40}N_4O_{10}$: C 45.66, H 4.03, N 5.60; found: C 45.58, H 4.14, N 5.57.

Crystallography: X-ray diffraction data were collected on an Enraf-Nonius CAD4 four-circle diffractometer. Corrections for Lorentz and polarization effects and for absorption (ψ scan) were applied. The crystal structure of the compound was solved by direct methods using the SIR97 program,[25] which gave the positions of all non-hydrogen atoms, although some of the fluorine atoms were later identified by successive Fourier difference syntheses. The structure was refined with the SHELX97 program package against F^2 with full-matrix least-square techniques.[26] Refinement of 596 parameters gave $R1 = 0.0630$ for 5677 reflections with $Fo > 4\sigma(Fo)$ and 0.0919 for all 7692 data with $S = 1.021$. The hydrogen atoms were calculated at fixed positions and refined with an overall isotropic thermal parameter.

Crystallographic data (excluding structure factors) have been deposited with the Cambridge Crystallographic Data Centre as supplementary publication no. CCDC-164371 (**2**). Copies of the data can be obtained free of charge on application to CCDC, 12 Union Road, Cambridge CB21EZ, UK (fax:(+44) 1223-336-033; e-mail:deposit@ccdc.cam.ac.uk).

Physical measurements: Magnetic studies where performed on powders and oriented single crystals in a Cryogenics S600 SQUID magnetometer. EPR spectra of both powder and single-crystal samples were performed with a Varian ESR9 spectrometer equipped with a helium flow cryostat at the X-band frequency.

Acknowledgements

Financial support by MURST and CNR, and by the EC through the TMR programs 3MD (no. ERB4061PL97-0197) and MOLNANOMAG (no. HPRN-CT-1999-0012) is acknowledged.

---

[1] G. Christou, D. Gatteschi, D. N. Hendrickson, R. Sessoli, *MRS Bulletin* **2000**, *25*, 66–71.

[2] R. Sessoli, D. Gatteschi, A. Caneschi, M. A. Novak, *Nature* **1993**, *365*, 141–3.

[3] L. Thomas, F. Lionti, R. Ballou, D. Gatteschi, R. Sessoli, B. Barbara, *Nature* **1996**, *383*, 145–147.

[4] J. R. Friedman, M. P. Sarachik, J. Tejada, R. Ziolo, *Phys. Rev. Lett.* **1996**, *76*, 3830–3833.

[5] W. Wernsdorfer, R. Sessoli, *Science* **1999**, *284*, 133–135.

[6] T. Lis, *Acta Crystallogr. B* **1980**, *36*, 2042–2046.

[7] Z. M. Sun, D. Ruiz, E. Rumberger, C. D. Incarvito, K. Folting, A. L. Rheingold, G. Christou, D. N. Hendrickson, *Inorg. Chem.* **1998**, *37*, 4758–4759.

[8] S. M. J. Aubin, Z. M. Sun, I. A. Guzei, A. L. Rheingold, G. Christou, D. N. Hendrickson, *Chem. Commun.* **1997**, 2239–2240.

[9] R. J. Glauber, *J. Mathem. Physics* **1963**, *4*, 294–307.

[10] A. Caneschi, D. Gatteschi, N. Lalioti, C. Sangregorio, R. Sessoli, *J. Chem. Soc. Dalton Trans.* **2000**, 3907–3912.

[11] A. Caneschi, D. Gatteschi, N. Lalioti, C. Sangregorio, R. Sessoli, G. Venturi, A. Vindigni, A. Rettori, M. G. Pini, M. A. Novak, *Angew.*

Chem. **2001**, *113*, 1810–1813; *Angew. Chem. Int. Ed.* **2001**, *40*, 1760–1763.

[12] A. Caneschi, D. Gatteschi, N. Lalioti, C. Sangregorio, R. Sessoli, G. Venturi, A. Vindigni, A. Rettori, M. G. Pini, M. A. Novak, *Europhys Lett.* submitted (available on the website http://ttt.lanl.gov/ps/cond-mat/0106224).

[13] A. Abragam, B. Bleaney, *Electron Paramagnetic Resonance of Transition Ions*, Dover, New York, **1986**.

[14] H. Andres, J. M. Clemente-Juan, R. Basler, M. Aebersold, H. U. Güdel, J. J. Borras-Almenar, A. Gaita, E. Coronado, H. Buttner, S. Janssen, *Inorg. Chem.* **2001**, *40*, 1943–1950.

[15] The distance *d* is calculated between the centroid of the five atoms of the hfac ligand (OCCCO) and the centroid of the phenyl ring of the radical.

[16] A. Bencini, D. Gatteschi, *Trans. Metal Chem.* **1982**, *8*, 1.

[17] J. R. Pilbrow, *Transition Ion Electron Paramagnetic Resonance*, Oxford University Press, Oxford, **1990**.

[18] A. Caneschi, D. Gatteschi, R. Sessoli, S. K. Hoffmann, J. Laugier, P. Rey, *Inorg. Chem.* **1988**, *27*, 2390.

[19] L. Banci, A. Bencini, C. Benelli, D. Gatteschi, C. Zanchini, *Struct. Bonding (Berlin)* **1982**, *52*, 37.

[20] A. Bencini, C. Benelli, D. Gatteschi, *Coord. Chem. Rev.* **1984**, *60*, 131.

[21] A. Bencini, C. Benelli, D. Gatteschi, C. Zanchini, *Inorg. Chem.* **1980**, *19*, 3027.

[22] A. Bencini, I. Ciofini, M. G. Uytterhoeven, *Inorg. Chim. Acta* **1998**, *274*, 90.

[23] M. G. F. Vaz, L. M. M. Pinheiro, H. O. Stumpf, A. F. C. Alcantara, S. Golhen, L. Ouahab, O. Cador, C. Mathoniere, O. Kahn, *Chem. Eur. J.* **1999**, *5*, 1486–1495.

[24] A. Caneschi, D. Gatteschi, P. Rey, R. Sessoli, *Inorg. Chem.* **1991**, *30*, 3936.

[25] A. Altomare, M. C. Burla, M. Camalli, G. Cascarano, C. Giacovazzo, A. Guagliardi, A. G. G. Moliterni, G. Polidori, R. Spagna, *J. Appl. Cryst.* **1999**, *32*, 115–119.

[26] G. M. Sheldrick, SHELX-97, an integrated system for solving and refining crystal structures from diffraction data, University of Göttingen (Germany), **1997**.

Received: July 3, 2001 [F3391]